Turkish Journal of Earth Sciences (Turkish J. Earth Sci.), **Vol. 16**, 2007, pp. 339–362. *Copyright ©TÜBİTAK*

Petrography, Geochemistry and Origin of Lower Liassic Dolomites in the Aydıncık Area, Mersin, Southern Turkey

MUHSİN EREN[1], MERYEM YEŞİLOT KAPLAN[1] & SELAHATTİN KADİR[2]

[1] Mersin Üniversitesi, Mühendislik Fakültesi, Jeoloji Mühendisliği Bölümü,
Çiftlikköy, TR–33343 Mersin, Turkey (E-mail: m_eren@yahoo.com)
[2] Eskişehir Osmangazi Üniversitesi, Mühendislik Mimarlık Fakültesi, Jeoloji Mühendisliği Bölümü,
Meşelik, TR–26480 Eskişehir, Turkey

Abstract: In the Aydıncık area, the Lower Liassic carbonates consist predominantly of dolomites, including limestone and dolomitic limestone intervals. These carbonates were deposited in peritidal environments, and later underwent early and late stage dolomitization. Petrographically, three dolomite-types are determined: (1) very fine to fine crystalline dolomite (T1) with crystal size of 13–65 μm and a good fabric preservation, (2) coarse crystalline sucrosic dolomite (T2) with size of 65 to 270 μm and fabric destruction, and (3) dolomite cement (T3) that occurs as a clear outer rim to cloudy coarse dolomite crystals (T2) or as a pore-lining and cement-fill of fenestral pores. The T1-type dolomites characterize the early stage of dolomitization formed from seawater by syn-sedimentary replacement of peritidal sediments. T2-type dolomites are derived from T1-type dolomites by recrystallization at increased burial temperature of ~50 °C. T3-type dolomites are precipitated as a cement from the same dolomitizing fluid. The recrystallization caused changes in texture, crystal ordering, isotope compositions and trace element contents. X-ray diffraction data indicates that the recrystallized dolomite (T2) is slightly better ordered and less calcium-rich than early dolomites (T1). More negative $\delta^{18}O$ values and lower Sr contents of the coarse crystalline dolomites (T2) reflect an equilibration with late diagenetic fluid during the recrystallization. The covariant trend between $\delta^{18}O$ and Sr values of T2-type dolomites shows an inverse relationship with their crystal size, suggesting progressive recrystallization. The $\delta^{13}C$ values of both dolomites are almost in the same range indicating the typical marine values that suggest little modification during late dolomitization. The T2-type dolomite geometry pinching out to the southward indicates an invasion of dolomitizing fluid from the north to the seaward into the platform carbonates, as a result of early compaction.

Key Words: dolomitization, burial, replacement, recrystallization, Liassic, Turkey

Aydıncık Yöresinde (Mersin, Güney Türkiye) Alt Liyas Dolomitlerinin Petrografisi, Jeokimyası ve Kökeni

Özet: Aydıncık yöresinde Alt Liyas karbonatları hakim olarak kireçtaşı ve dolomitik kireçtaşı ara seviyeleri içeren dolomitlerden oluşur. Bu karbonatlar gel-git çevresi ortamında çökelmiş ve daha sonra erken ve geç evre dolomitleşmesine uğramıştır. Petrografik olarak üç tip dolomit belirlenmiştir: (1) 13–65 μm kristal boyutlu ve iyi doku korunmalı çok ince ile ince kristalli dolomit (T1); (2) 65–270 μm kristal boyutlu ve doku korunmasız iri kristalli şeker dokulu dolomit (T2); ve (3) bulanık iri dolomit kristalleri (T2) çevresinde açık dış kenar veya fenestral gözenekleri çevreleyen ve çimento dolgusu olarak görülen dolomit çimento (T3). T1-tip dolomitler gel-git çevresi çökellerin çökelmeyle yaşıt ornatımıyla deniz suyundan oluşmuş erken evreyi karakterize eder. Daha sonra T2-tip dolomitler yaklaşık 50 °C gömülme sıcaklığında T1-tip dolomitlerin yeniden kristallenmesiyle oluşmuştur ve T3-dolomitler aynı dolomitleşme sıvısından çimento olarak çökelmiştir. Yeniden kristallenme erken evre dolomitlerinin dokusunda, kristallenme derecesinde, izotop kimyasında ve iz element içeriğinde değişimlere neden olmuştur. X-ışını difraksiyonu verileri yeniden kristallenme dolomitlerinin (T2) erken dolomitlere (T1) göre hafifçe daha iyi kristallenmeli ve daha az kalsiyum içerikli olduğunu gösterir. İri kristalli dolomitlerin (T2) daha negatif $\delta^{18}O$ değerleri ve düşük Sr içerikleri yeniden kristallenme sırasında diyajenetik sıvı ile dengeyi yansıtır. T2-dolomit örneklerinin $\delta^{18}O$ ve Sr değerlerinin birlikte değişim eğilimi ilerleyici yeniden kristallenmeyi destekler şekilde kristal boyutuyla ters bir ilişkiyi gösterir. Dolomitlerin $\delta^{13}C$ değerleri hemen hemen aynıdır ve dolomitleşme sırasında çok az değişim gösteren tipik denizel değerleri gösterir. T2-dolomitlerinin güneye doğru kapanan geometrisi, dolomitleşme sıvısının erken sıkışma sonucu olarak kuzeyden güneye platform karbonatlarının içine ilerlediğini gösterir.

Anahtar Sözcükler: dolomitleşme, gömülme, ornatma, yeniden kristallenme, Liyas, Türkiye

Introduction

The study area is located in the Aydıncık (Mersin) district which is known as a part of the central Taurides in southern Turkey (Özgül 1984; Figure 1). The Tauride mountains consist mostly of platform carbonates deposited during Palaeozoic and Mesozoic time. In the central Taurides, the Mesozoic platform carbonates are represented by the Cehennemdere Formation (Demirtaşlı *et al.* 1984). The lower most part of the Cehennemdere Formation is made up predominantly of Lower Liassic platform dolomites. There is a little information available concerning dolomitization in either the study area or Tauride platform carbonates in southern Turkey. The recent detailed study has been published by Varol & Matsumoto (2005) that provides an information about Middle Devonian platform dolomites of the Tauride mountains. Therefore, this study aims to determine petrographic and geochemical features of the Lower Liassic dolomites in the Aydıncık area, and proposes a model to explain their occurence.

In contrast to Turkey, there are numerous studies in the world from different locations, particularly concerning the pervasive dolomitization of platform carbonates and associated reefs (e.g., Theriault & Hutcheon 1987; Zengzhao *et al.* 1998; Reinhold 1998; Balog *et al.* 1999; Qing *et al.* 2001; Haas & Demeny 2002; Auajjar & Boulegue 2003). Many platform carbonates and associated reefs show two major stages of dolomitization: (1) early stage (syn-sedimentary) – characterized by generally very fine to fine crystalline dolomites with good fabric preservation, and (2) post-depositional stage, represented by medium to coarse crystalline dolomites with fabric destruction (Morrow 1982). Most authors agree that the early dolomites form by replacement of the precursor sediments soon after deposition from evaporative or normal marine waters (Theriault & Hutcheon 1987; Carballo *et al.* 1987; Budd 1997; Zengzhao *et al.* 1998; Yoo & Lee 1998; Qing 1998; Qing *et al.* 2001; Varol & Matsumoto 2005). In the platform carbonates, the post-depositional or burial stage is commonly characterized by the recrystallization and subsequent chemical alteration (neomorphic alteration) of the early-formed metastable dolomites (Land 1985; Morrow 1982). The recrystallization results textural, crystallographic and geochemical changes (Land 1985; Machel 1997). This study confirms a similar diagenetic evolution for the Lower Liassic platform carbonates.

Geological Setting

Turkey has been subdivided geologically into four major tectonic units, namely the Pontides, Anatolides, Taurides and Border folds (Ketin 1966). The Taurides extend on east–west direction, subparallel to the coastline of the Mediterranean Sea, and represent a part of the Alpine orogenic system in southern Turkey (Figure 1a). In Turkey, the Alpine orogenic system is a product of the destruction of Tethys (Adamia *et al.* 1980; Şengör & Yılmaz 1981; Şengör *et al.* 1984). In the Mesozoic time, the Tethyan domain between African-Arabian and Laurasia consisted of two oceans, separated by a string of continental fragments (Dewey *et al.* 1973). The northern ocean has been named the Palaeotethys, and southern ocean the Neotethys.

The Late Mesozoic–Cenozoic evolution of the Taurides was controlled by tectonic events which caused the opening and closing of the Neotethys (Şengör & Yılmaz 1981). The evolution of the Neotethys has been summarised by Robertson (1998). The Neotethys was formed by continental rifting in the Triassic, followed by a passive margin history during the Jurassic–Early Cretaceous, and the genesis and emplacement of ophiolites in the Late Cretaceous. A remnant of the Neotethys survived into the Early Tertiary times (with localised subduction/accretion and arc volcanism), until initial continental collision. The collision was completed by Middle to Late Miocene time, followed by a switch to strike-slip and the westward tectonic escape of Anatolia.

The Tauride carbonate platform, developed on the passive margin, is considered either as an independent continental block, separated during Mesozoic time from the African-Arabian continent by an oceanic basin, or as an integral part of the African-Arabian continent with the only ocean basin being situated to the north of it (Dewey *et al.* 1973).

In the Aydıncık area, a thick sedimentary pile ranging in age from the Infra-Cambrian (Precambrian) to the Recent is present (Figures 2 & 3). The Jurassic to Lower Cretaceous Cehennemdere Formation, first named by Demirtaşlı *et al.* (1984), is situated in the middle of this thick sedimentary succession (Figure 3). The general geological studies have been carried out by Yüksel (1985), Koç (1996) and Koç *et al.* (1997, 2005) who subdivided the Cehennemdere Formation into three members. These are the Dibekli Member (mostly

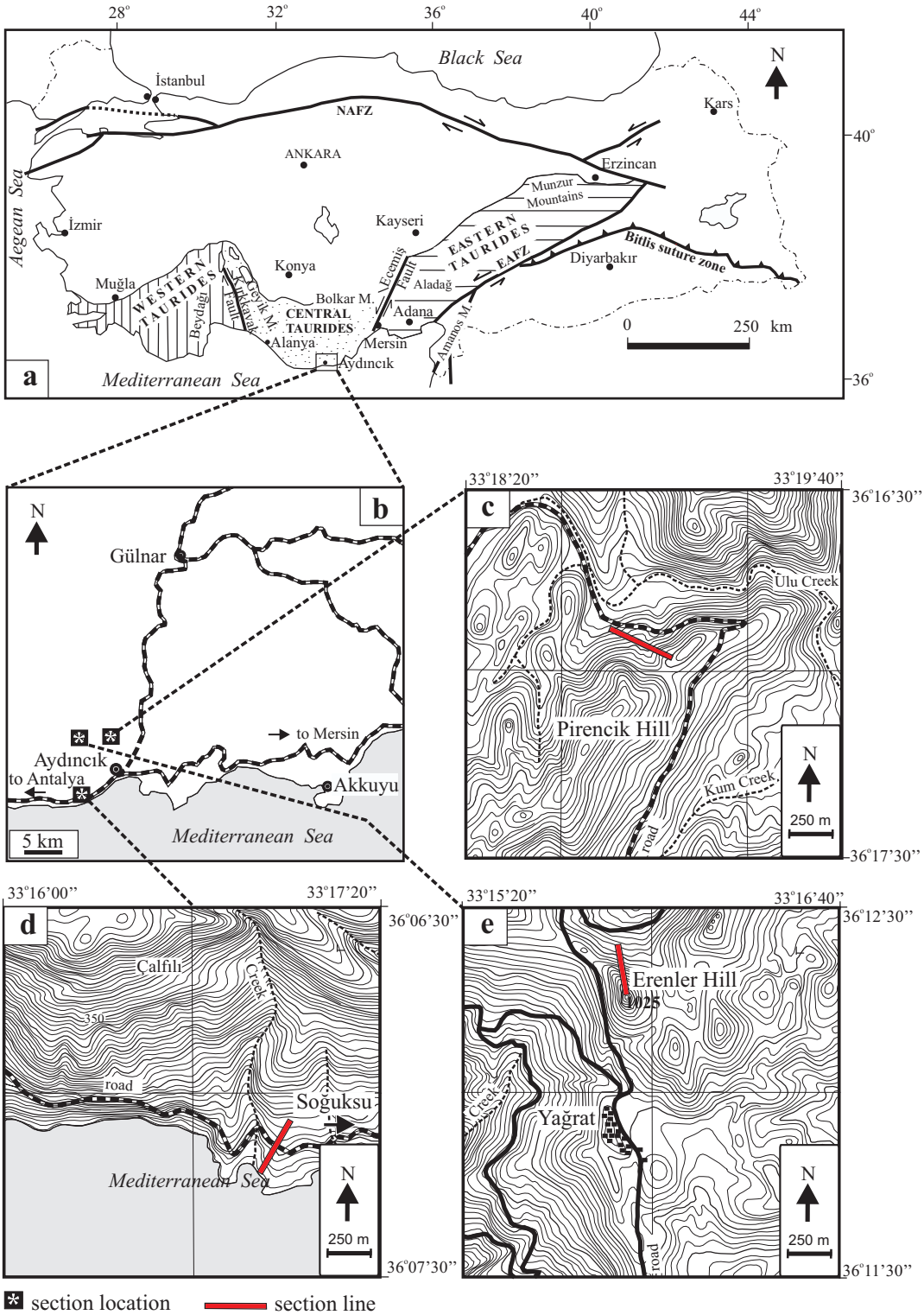

Figure 1. (a) A schematic map illustrating the Tauride Orogenic Belt and its subdivisions (modified from Özgül 1984; major faults from Bozkurt 2001); (b) location map of the measured sections; (c), (d), (e) topographic maps showing the positions of the measured sections of Pirencik hill, Erenler hill and Soğuksu location, respectively. NAFZ– North Anatolian Fault Zone, EAFZ– East Anatolian Fault Zone, M– Mountain.

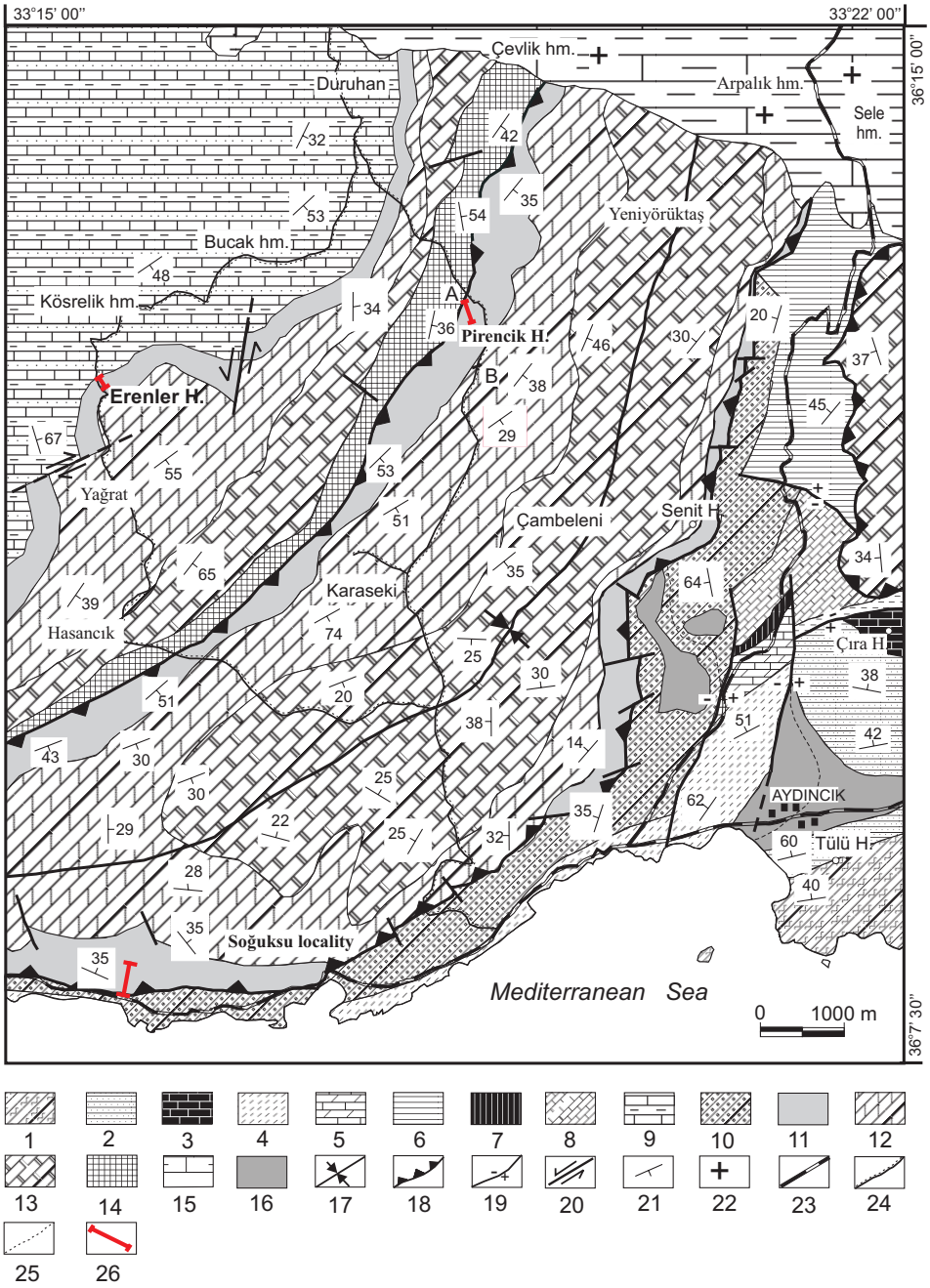

Figure 2. Geological map of the Aydıncık (Mersin) area (modified from Koç *et al.* 1997). 1– Sipahili Formation (Infra-Cambrian); 2– Hüdai Quartzite (Early Cambrian); 3– Çaltepe Formation (Early to Middle Cambrian); 4– Seydişehir Formation (Late Cambrian to Ordovician); 5– Büyükeceli Formation (Middle Devonian); 6– Akdere Formation (Late Devonian); 7– Korucuk Formation (Early Carboniferous); 8– Kırtıldağı Formation (Late Permian); 9– Late Palaeozoic (undifferentiated units); 10– Murtçukuru Formation (Late Triassic); 11 to 13– Cehennemdere Formation: 11– Dibekli member (Liassic to Dogger ?), 12– Örendüzü member (Dogger–Early Cretaceous ?), 13– Çambeleni member (Early Cretaceous); 14– Yavca Formation (Late Cretaceous); 15– Mut Formation (Middle Miocene); 16– alluvium and alluvial terrace (Quaternary); 17– syncline axis; 18– thrust fault; 19– normal fault; 20– strike-slip fault; 21– strike and dip of bedding; 22– horizontal bed; 23– main road; 24– stabilized road; 25– stream; 26– measured section line.

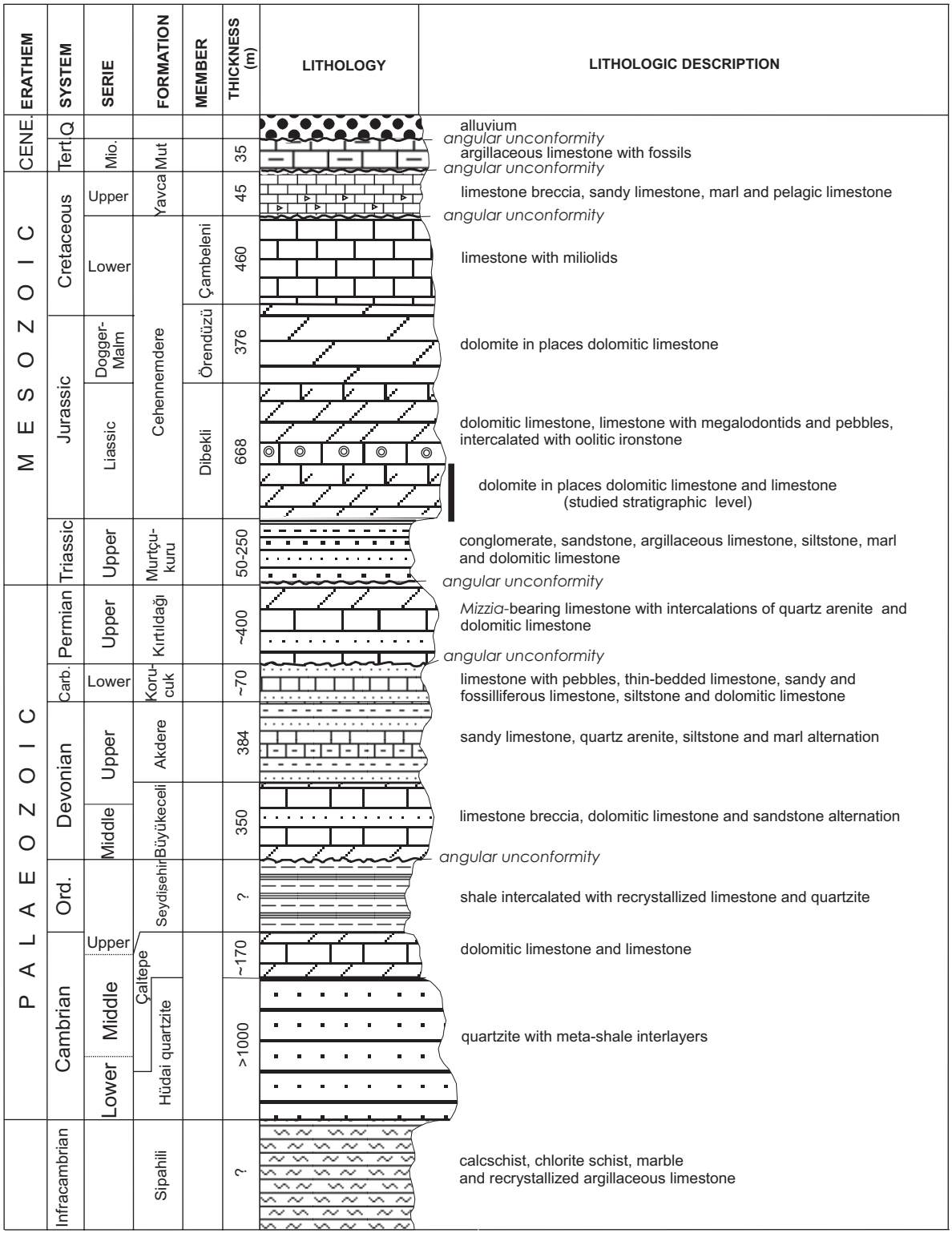

Figure 3. Generalized stratigraphic column of the Aydıncık area (modified from Koç *et al.* 1997).

Liassic–Dogger?) comprising dolomite, microbially laminated limestone, and cyclic carbonates (Eren *et al.* 2002; Kabal & Taslı 2003); the Örendüzü Member (Dogger–Early Cretaceous) consisting predominantly of dolomite and dolomitic limestones, and the Çambeleni Member (Early Cretaceous) composed mainly of miliolid-bearing limestones (Yüksel 1985; Koç 1996). Yeşilot (2005) provides early information on the Lower Liassic dolomites in the area, which is the base for this study. The lower part of the Liassic carbonates either lack fossils or contain few fossils because of extensive dolomitization, so that its age is uncertain and the nature of the lower boundary of the Liassic carbonates remains obscured. Biostratigraphic details are provided by Kabal & Taslı (2003), based on the benthic foraminifera. The upper boundary of the Lower Liassic carbonates is marked by a zone, taking place between the *Orbitopsella* zone (Upper Sinemurian to Lower Pliensbachian) and *Lituosepta recoarensis* zone (Upper Sinemurian). The marker zone roughly corresponds to the lower boundary of the cyclic carbonates which is easily recognizable on the field. The carbonates below the *Lituosepta recoarensis* zone with scarce *Siphovalvulina* sp. are attributed to Hettangian–Lower Sinemurian time because the genus *Siphovalvulina* is a Jurassic form.

Methodology

During the field work, three measured-sections were surveyed at Pirencik hill, Erenler hill, and Soğuksu location (Figure 1). A total of 128 samples were collected from the three sections. Thin-sections were prepared from each sample, and were stained with a mixture of alizarin red S and potassium ferricyanide to differentiate calcite from dolomite and their ferroan and non-ferroan phases (Dickson 1966). All thin-sections were examined under an optical microscope. Representative carbonate samples were analyzed for their mineralogical characteristics by X-ray powder diffractometry (XRD) (Rigaku-Geigerflex) and scanning electron microscopy (SEM-EDX) (JEOL JSM 84A-EDX). XRD analyses were performed using CuKa radiation and a scanning speed of 1° 2θ/min to determine mineralogical composition of the bulk samples. Semi-quantitative mineral abundances are obtained by multiplying the basal peak intensities of each mineral by suitable factors according to a method represented by Brindley (1980) and later modified by Gündoğdu (1982). In this method, the relative error is less than 15% (Gündoğdu 1982). Estimation of the ordering degree in dolomites is based on the ratio of the intensities of the d_{015} to d_{110} (hexagonal index) peaks (Hardy & Tucker 1995). Furthermore, crystal ordering of dolomites is obtained from a ratio between d_{015} and d_{110} peak heights with a standard deviation (σ) of 0.11 for very fine to fine crystalline dolomites (T1-type) and 0.19 for coarse crystalline dolomites (T2-type). Representative dolomite samples were prepared for SEM-EDX analysis by adhering the fresh, broken surface of the sample on to an aluminium sample holder with double-sided tape and thinly coating with a film (~350 Å) of gold using a Giko ion coater.

Chemical composition of selected samples were determined using inductively coupled plasma atomic emission spectroscopy (ICP-AES) analyses, and were carried out at the ACME Analytical Laboratories LTD., Vancouver, BC (Canada). In these analyses, experimental error is less than ±0.04 wt% for major elements, and less than ±5 ppm for trace elements. The mole % $MgCO_3$ content of dolomite is determined using the result of geochemical analyses. Sample selection for stable isotope analyses was based on detailed petrography, XRD and ICP-AES analyses. A Finigan MAT 252 mass spectrometer, Southern Methodist University (SMU), Dallas, TX, USA has been used for oxygen and carbon analysis. 5–10 mg powdered carbonate samples reacted with 100% phosphoric acid (H_3PO_4) at 50 $^{\circ}$C for dolomites and 25 $^{\circ}$C for calcite. The acid fractionation factors (α) are 1.010250 for calcite and 1.011091 for dolomite. Replicate analyses on the randomly selected samples give a mean deviation of ±0.057 ‰ for $\delta^{18}O$ and ±0.02 ‰ for $\delta^{13}C$. All isotope data are reported in per mill (‰) with repect to the PDB standard.

Lower Liassic Dolomites

Field Description

The field description of dolomites is based on the three sections (Figures 1, 4–7). The thickness of the Lower Liassic carbonates is measured approximately 281 m at Pirencik hill, 248 m at Erenler hill and 247 m at Soğuksu location. In the sections, Lower Liassic carbonates are conformably overlain by Upper Liassic cyclic carbonates consisting of intraformational conglomerate, Megalodont *Orbitopsella*-bearing micritic limestone and microbially laminated limestone (Eren *et al.* 2002). At the Soğuksu

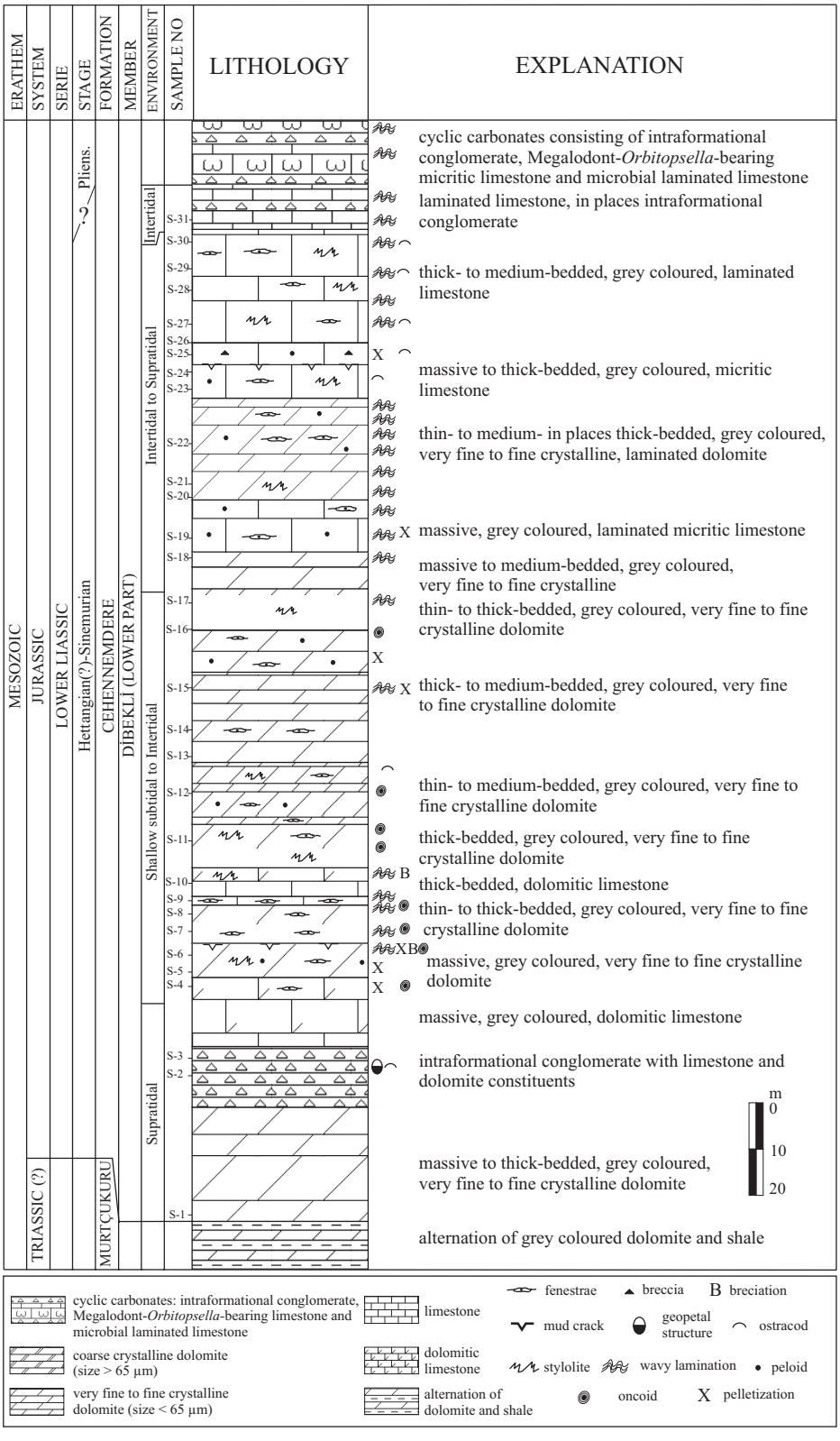

Figure 4. The Soğuksu measured stratigraphic section (see Figures 1d & 2 for location).

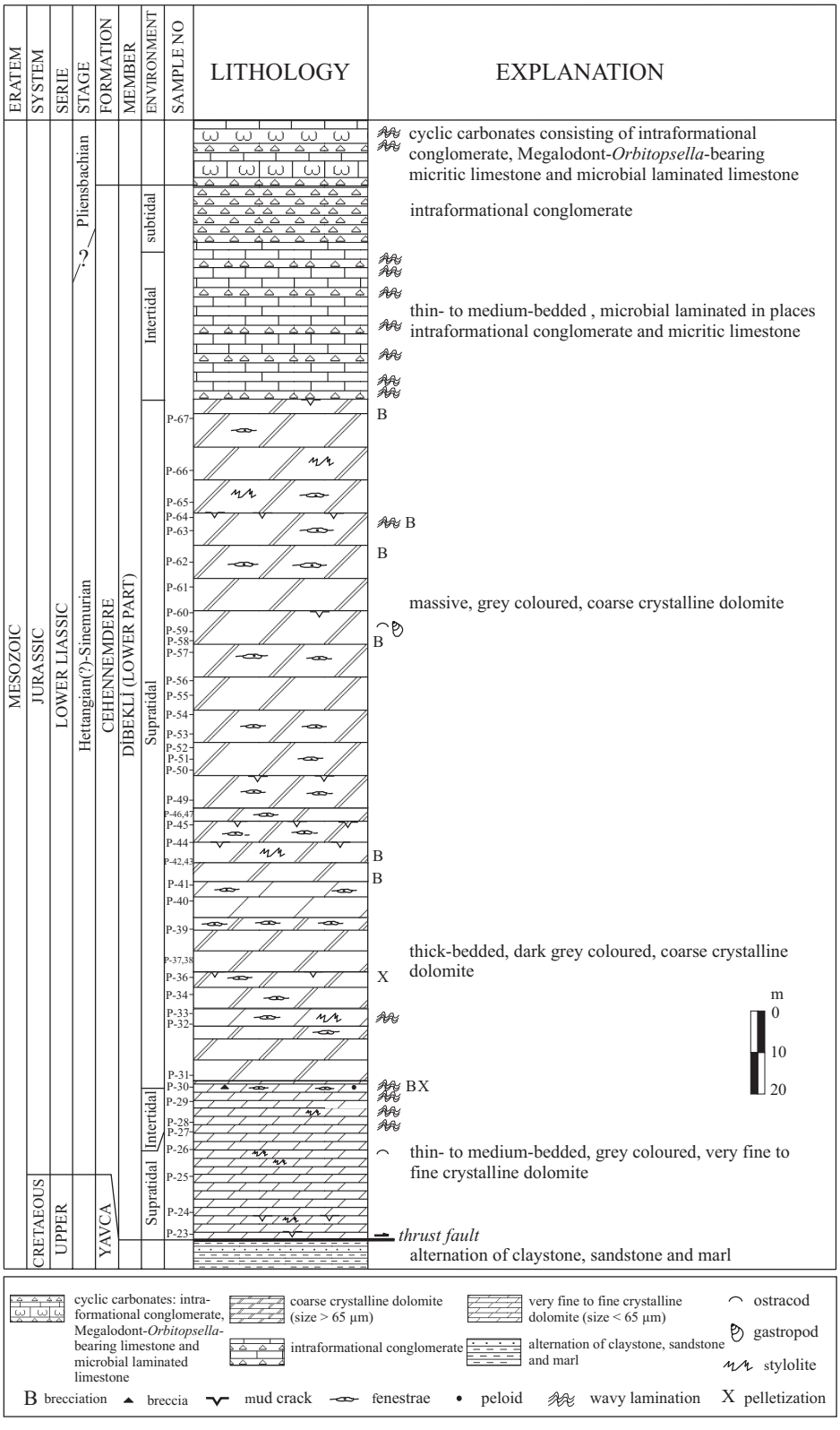

Figure 5. The Pirencik hill measured stratigraphic section (see Figures 1c & 2 for location).

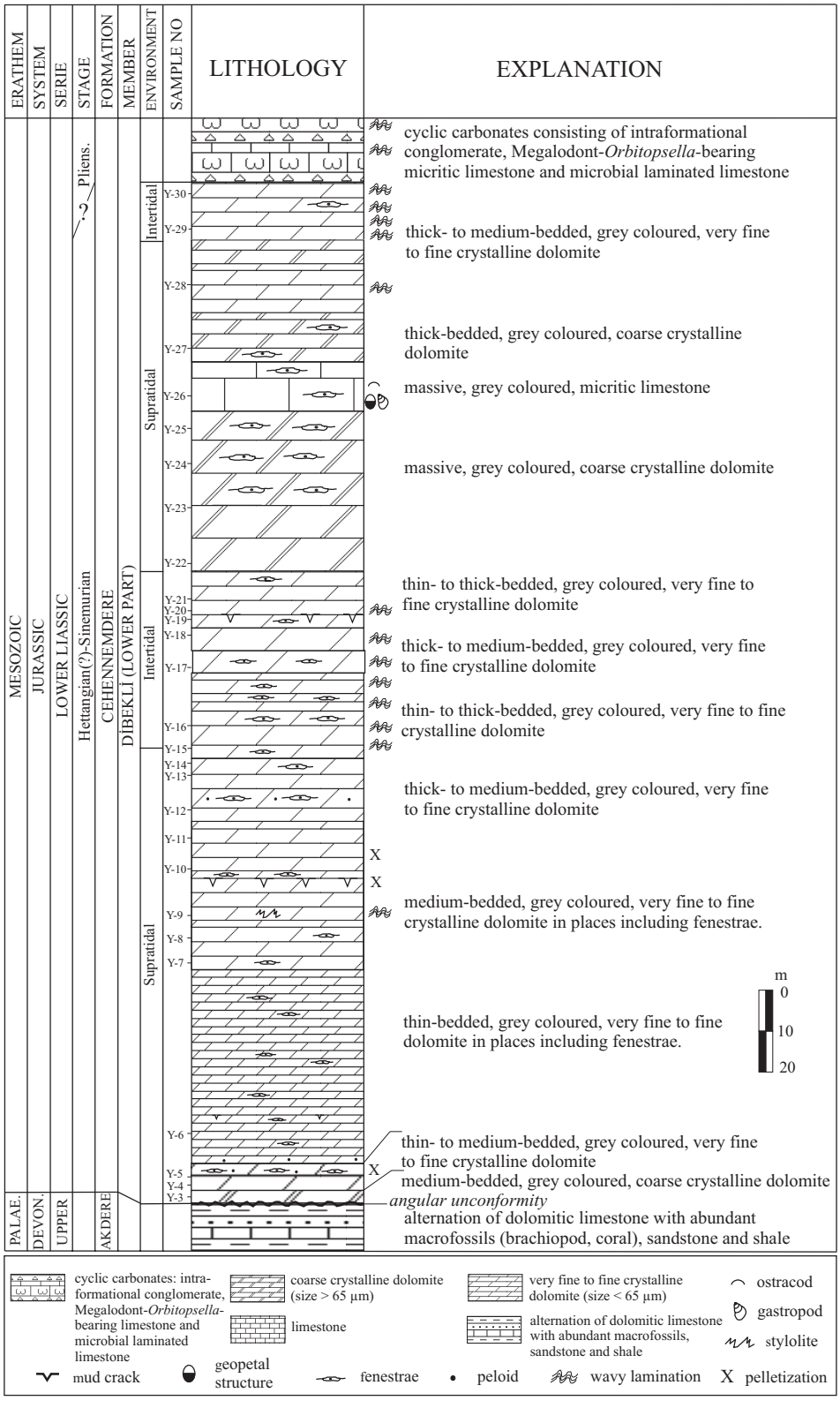

Figure 6. The Erenler hill measured stratigraphic section (see Figures 1e & 2 for location).

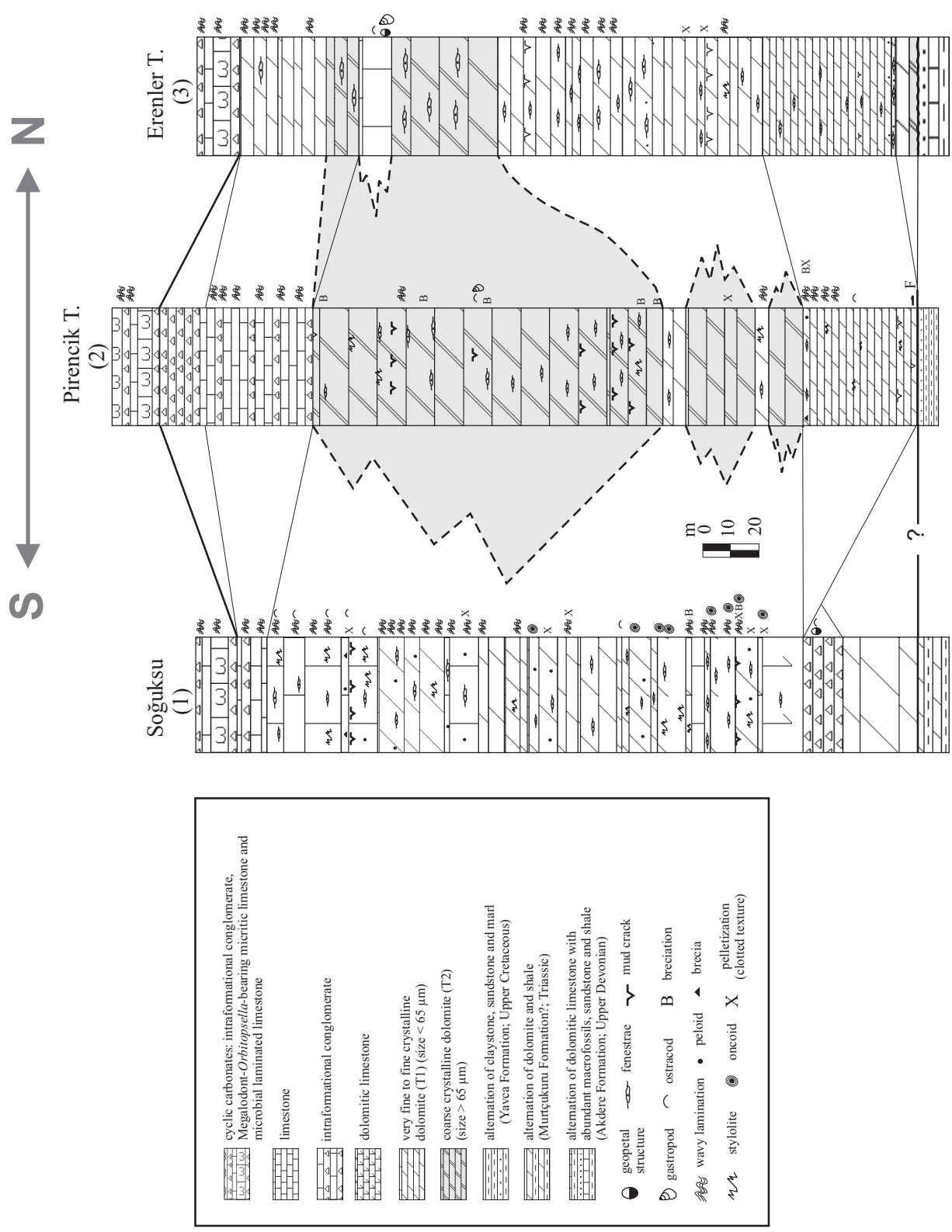

Figure 7. A correlation of the measured sections and spatial distribution of two major dolomite-types.

location, situated on the southern flank of a syncline (Figure 2), Lower Liassic carbonates conformably overlie Triassic sediments of the Murtçukuru Formation composed of dolomites and clastic sediments (Kabal & Taslı 2003). At Pirencik hill, located on the northern flank of the syncline, Lower Liassic dolomites tectonically overlie the Upper Cretaceous sediments of the Yavca Formation along a thrust fault. At Erenler hill, Lower Liassic carbonates unconformably overlie Upper Devonian sediments of the Akdere Formation which consists of brachiopod-bearing limestone, quartz-arenite, siltstone and shale alternation. On the field, Lower Liassic dolomites are typically grey in colour and often have a coarsely crystalline sucrosic texture. The bed-thickness is variable, but massive and thick-bedding are common.

Petrography

Petrographic examination reveals that the dolomite occurs in three modes in the Lower Liassic carbonates. One of the most common modes is very fine to fine crystalline dolomite (T1; Figure 8) (predominantly 13–26 μm and up to 65 μm in size) replacing unfossilliferous or scarcely fossilliferous mudstone often with irregular fenestral voids, laminated mudstone-microbialite- and/or intraclast-peloid-bearing grainstone/packstone with laminoid or irregular fenestrae, and non-laminated intraclast-peloid bearing grainstone/packstone. Scarce fossils are mostly ostracod fragments and gastropods. Some peloidal packstones contain oncoids. This type of dolomite shows well-preserved textures of original sediments. Desiccation cracks, local microbrecciation and clotted textures are associated with these mud-supported carbonate rocks (Figure 8g, h). Late diagenetic stylolites are also present, and are parallel or subparallel to bedding planes.

The second type of dolomite (T2) is pervasive like the first type, but is fabric destructive, probably formed through recrystallization and/or replacement and consisting of coarse dolomite crystals (sucrosic dolomite; Figure 9) with a size of 65 to 130 μm, up to 270 μm. Both idiotopic and xenotopic textures are common. Some dolomite crystals have a larger size and clear rims (limpid) towards the pore centre (Land 1980; Morrow 1982; Qing 1998; Qing *et al.* 2001). In most cases, tiny crystals are observed in the cloudy central part of euhedral dolomite rhombs; they are probably relics of the first-type of dolomites after recrystallization. The rocks with a xenotopic texture seem to be a mosaic of anhedral dolomite crystals with a cloudy appearance and irregular crystal boundaries. In this type of dolomite, the relics of original fabrics are absent or sparse except for some traces of birds-eye structures and a few fossils. In addition, late diagenetic stylolites truncate the second type of dolomite crystals.

The third-type of dolomite (T3) is a cement precipitated in intercrystalline pores as a thin and clear outer rim or zone around a single or cluster of dolomite rhombs (second-type) as syntaxial overgrowths (Figure 10a, b) and also in some fenestral pores as pore-lining and space-filling crystals with variably large crystal sizes up to 700 μm (Figure 10c, d). The staining of the thin-sections with potassium ferricyanide reveals that both outer rim and pore-filling cements are nonferroan. The thickness of the rim cement is mostly 10–40 μm. The boundary between rim cement and coarse dolomite crystals (second-type) is gradational or sharp. The third type of dolomite is not as important volumetrically as the first (~60%) and second (~40%) types of dolomite, and accounts for 1–2% or less of the all dolomites.

Depositional Environment

The sedimentary characteristics of the Lower Liassic partly or completely dolomitized carbonates indicate deposition in a peritidal environment including predominantly intertidal and supratidal zones (Figures 4, 5 & 6). Lime mudstones with fenestral fabric, mudcracks and un- or sparsely fossiliferous content are quite common in supratidal environments and suggest low energy conditions. The abundance of mud cracks in Pirencik hill and Erenler hill sections (Figures 5 & 6) suggests that sediments there were frequently subjected to subaerial conditions. Finely laminated peritidal carbonates commonly associated with fenestral fabrics are characteristic of intertidal facies (Ginsburg 1975; Park 1976; Tucker & Wright 1990). The alternation of microbialite and micrite laminae with peloidal and small intraclast-rich laminae is resulted by the alternating tidal and storm floodings (Park 1976; Tucker & Wright 1990; Tucker 1991). The laminae, which usually contain peloids and small intraclasts or oncoids, are deposited during periods of storm flooding, whereas the microbialite and micrite laminae are formed during daily tidal flooding.

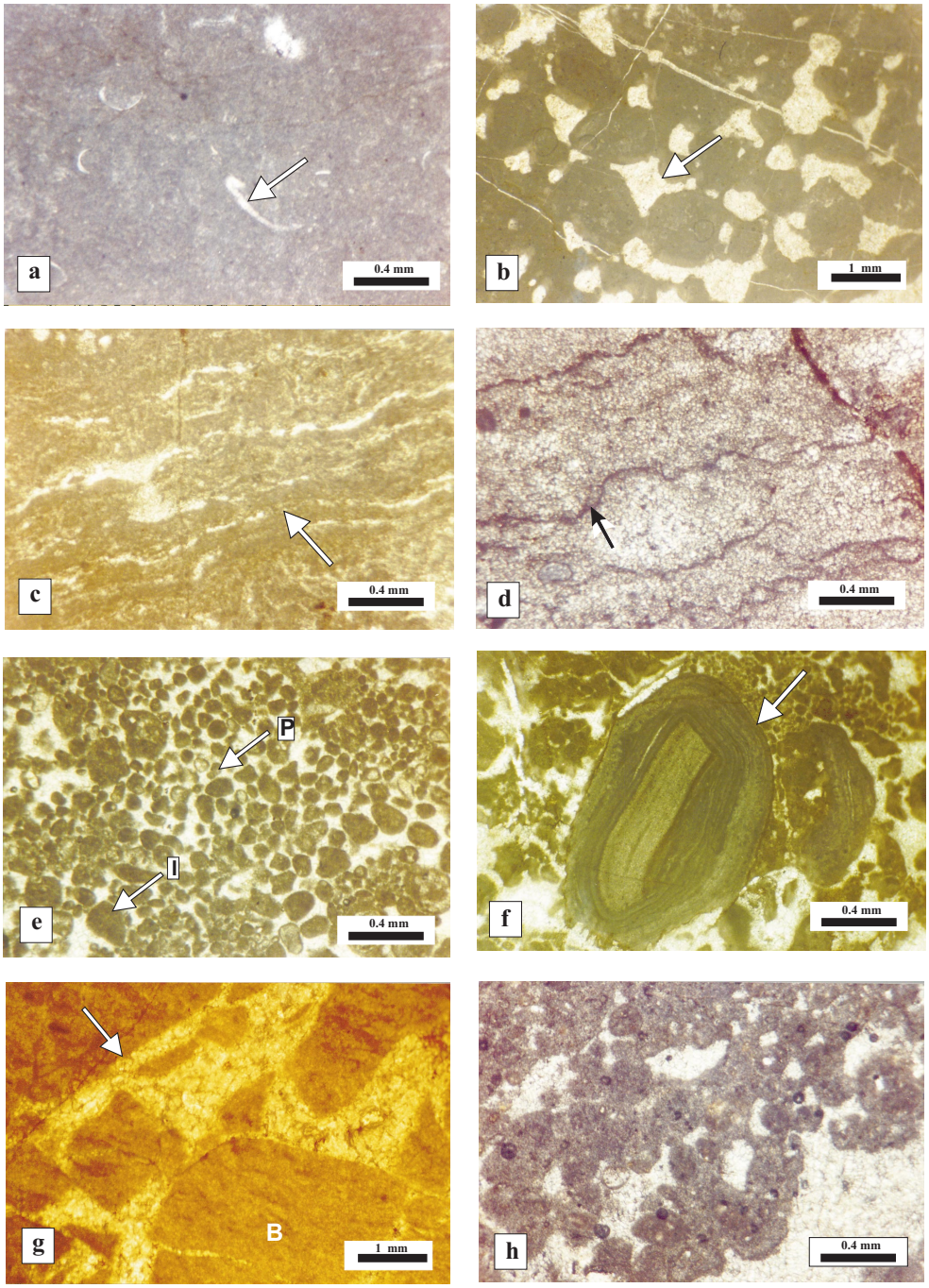

Figure 8. Photomicrographs showing characteristic textures and fabrics of host-sediments of early dolomites and associated limestone. **(a)** Very fine crystalline dolomite (T1) showing a well-preserved original sediment fabric of scarcely fossilliferous mudstone. Arrow illustrates a fragment of ostracod shell; **(b)** very fine crystalline dolomite (T1) replacing mudstone (micrite) with irregular fenestral pores (arrow); **(c)** fine laminated limestone associated with the early dolomites. Arrow shows lamina; **(d)** fine crystalline dolomite (T1) showing relics of original lamination (arrow); **(e)** very fine crystalline dolomite replacing small intraclast (I)-peloid (P) bearing grainstone; **(f)** very fine crystalline dolomite replacing oncoid-small intraclast-peloid bearing grainstone. Arrow shows an oncoid; **(g)** desiccation cracks (arrow) with fine crystalline dolomitic clasts (B); **(h)** very fine crystalline dolomite (T1) showing clotted texture of the original sediment.

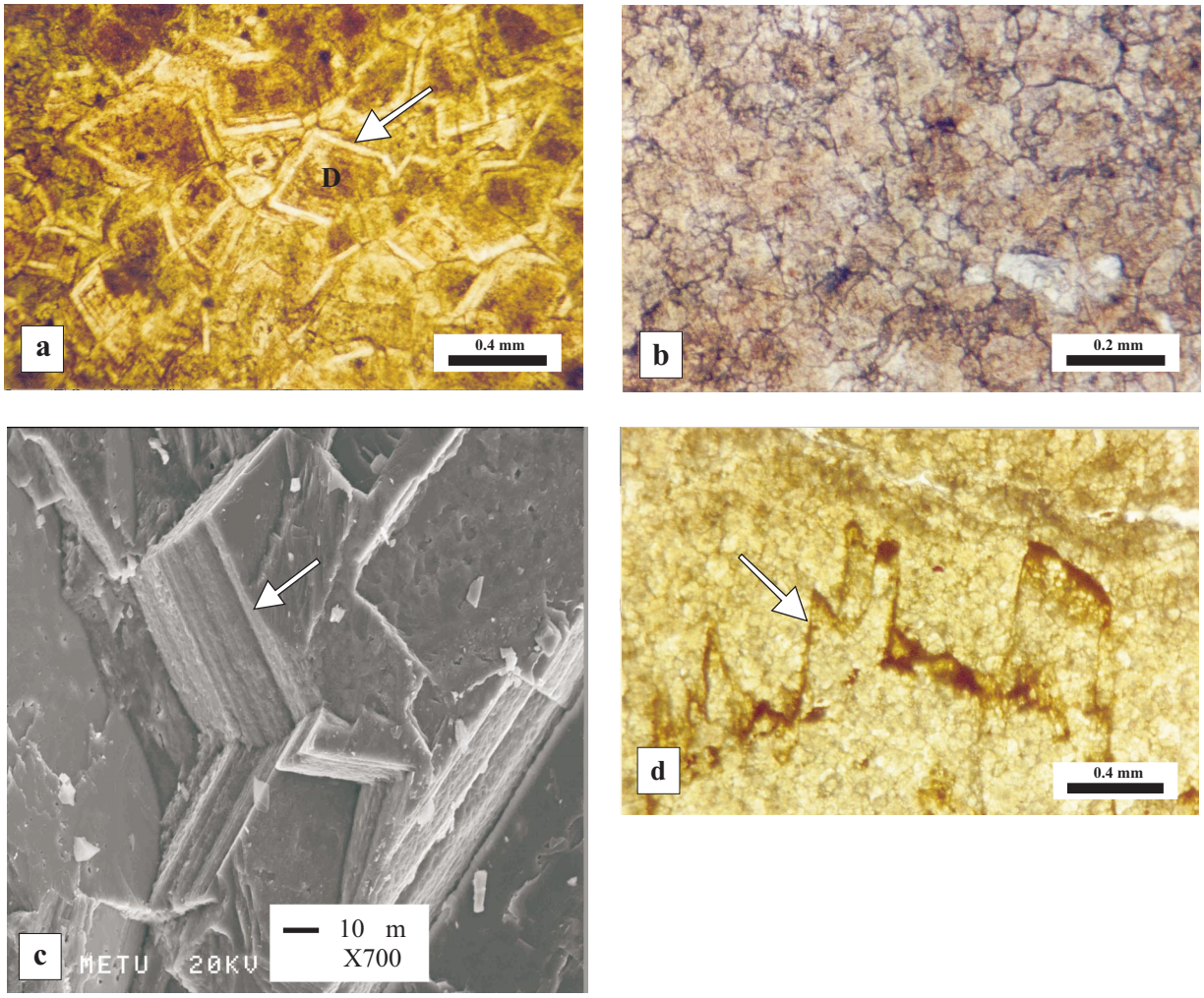

Figure 9. Photomicrographs and SEM view of second-type dolomites. **(a)** Photomicrograph of the coarse crystalline dolomite with an idiotopic texture. Most of the euhedral dolomite crystals show a clear outer cement-rim (arrow); **(b)** coarse crystalline dolomite with a xenotopic texture; **(c)** SEM view of an euhedral coarse dolomite crystal (arrow); **(d)** late diagenetic stylolite cutting the coarse dolomite crystals (T2).

Some oncoid-rich intraclast-peloid-bearing grainstone/packstone may indicate deposition in a shallow subtidal to lower intertidal environment (Halley 1975; Tucker & Wright 1990; Figure 4). Vertical and lateral facies changes in the sections (Figures 4–7) are interpreted as having been caused by the sea-level fluctuations and topography of the depositional environment slightly deepening to the south (Figure 7), respectively.

Mineralogy and Geochemistry

XRD Analysis. X-ray diffraction (XRD) analysis was used to determine carbonate mineralogy, semi-quantitative mineral abundance (Table 1) and crystal-ordering. Dolomite is dominant mineral associated with accessory calcite, and locally trace amount of quartz. Some samples consist mainly of calcite indicating the presence of undolomitized limestone levels (Table 1). The intensity ratios of the d_{015} to d_{110} peaks range from 0.40 to 0.80 (0.11 σ) for the T1-type dolomites and from 0.50 to 0.88 (0.19 σ) for the T2-type dolomites. These values demonstrate that all dolomites are poorly to moderately ordered and calcium-rich. The coarse crystalline dolomites show a sligthly better ordering with respect to the T1-type dolomites. The estimated average compositions of dolomites based on displacement of the

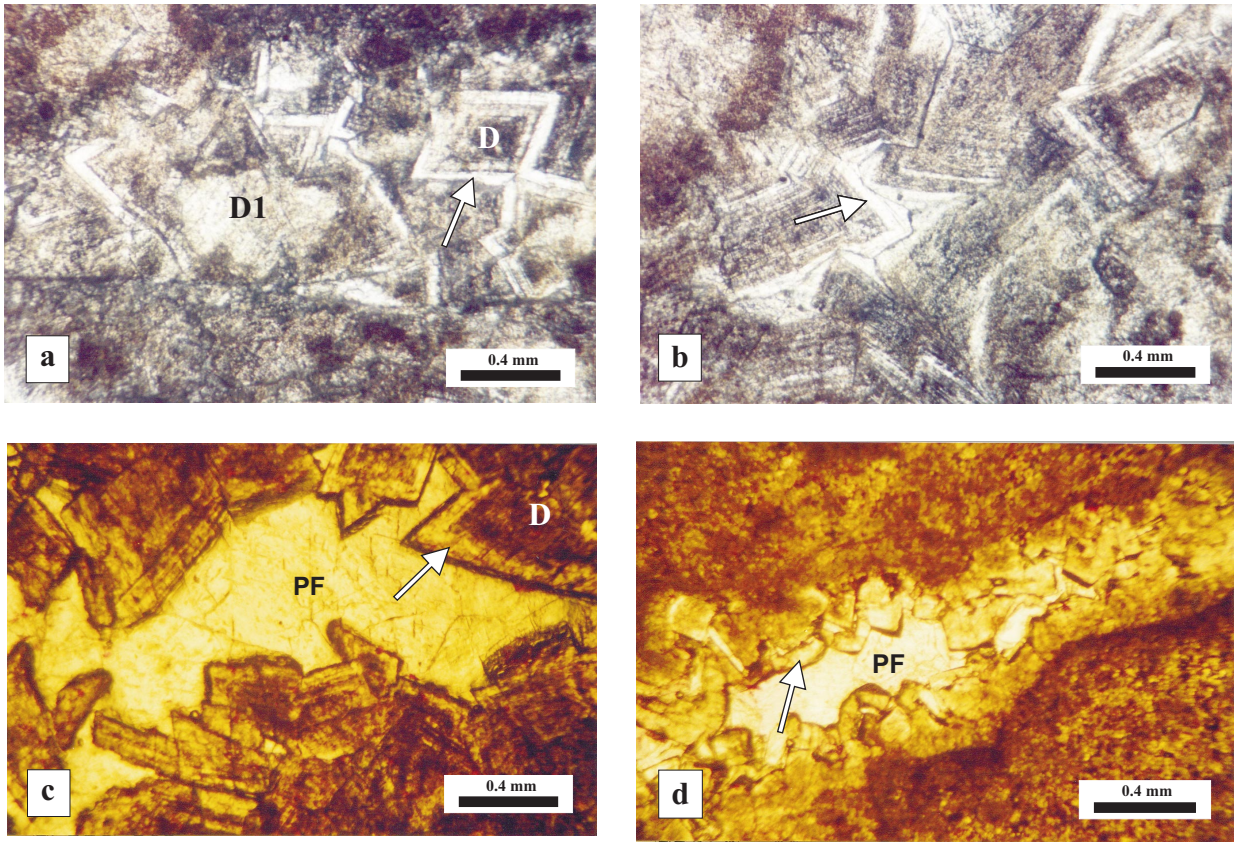

Figure 10. Photomicrographs of dolomite cements (third-type dolomite). **(a)** Dolomite cement (third-type dolomite) as clear outer rim around single (D) and clusters (D1) of dolomite rhombs (second-type); **(b)** dolomite rim-cement (third-type) lining the intercrystalline pore (arrow) in the coarse crystalline dolomite (second-type); **(c)** dolomite cement (third-type) lining (arrow) and filling (PF) a fenestral pore (?) in the coarse crystalline dolomite (D); **(d)** dolomite scalenohedral rim cement (arrow) and filling (PF) a fenestral pore

d_{104} peak of calcite (Goldsmith *et al.* 1961) are $Ca_{56.}$ Mg_{44} for the T1-type dolomite and $Ca_{55.}$ Mg_{45} for the T2-type dolomite.

ICP-AES Analysis. ICP-AES analyses were carried out on selected samples to determine the precise chemical composition of the dolomites and coexisting limestone, and the results are given in Table 2. The T1-type dolomites contain an average of 20.77 wt% in MgO, 31.10 wt% in CaO, and 84.7 ppm Sr. Whereas the T2-type dolomites have an average of 21.44 wt% in MgO, 31.42 wt% in CaO, and 57.44 ppm Sr. By comparison, the T2-type dolomites are slightly enriched in MgO content (~0.67 in wt%) and depleted in Sr (~27 ppm) relative to T1-type dolomites. In overall, the Sr values are considerably lower than modern marine dolomites (500–800 ppm Sr in Land 1980; ~600–700 ppm Sr in Behrens & Land 1972), which are due to neomorphic alteration during later burial diagenesis. The molar concentration of $MgCO_3$ calculated from the geochemical results averages 43.5 mole % for T1-type dolomites and 45 mole % for T2-type of dolomite. These values indicate that both T1- and T2-types are Ca-rich dolomites.

Stable Isotopes. The oxygen and carbon isotopic compositions of carbonate samples are listed in Table 3, and plotted in Figure 11. The bulk samples of T1-type dolomite show $\delta^{18}O$ and $\delta^{13}C$ values ranging from +0.21 to –1.79 ‰ PDB (avg. –0.52 ‰ PDB) and +1.12 to –0.58 ‰ PDB (avg. +0.23 ‰ PDB), respectively. The $\delta^{18}O$ and $\delta^{13}C$ values for T2-type dolomites are –1.27 to –3.44 ‰ PDB (avg. –2.80 ‰ PDB) and +1.16 to –0.26

Table 1. Semi-quantitative mineralogical compositions of the selected samples.

sample no	dolomite	calcite	quartz
P-23	+++++	-	
P-24	+++++	-	
P-25	+++++	-	
P-26	+++++	-	
P-28	+++++	ac	
P-29	+++++	ac	
P-31	+++++	ac	
P.33	+++++	ac	
P-34	+++++	-	
P-35	+++++	ac (~ 4%)	
P-36	+++++	ac (~ 3%)	
P-39	+++++	ac	ac
P-40	+++++	ac (~ 4%)	
P-41	++++	+ (~ 8%)	
P-42	+++++	ac	
P-43	+++++	ac	
P-44	+++++	ac	
P-46	+++++	-	
P-47	+++++	-	
P-48	+++++	ac	
P-49	+++++	-	
P-50	+++++	ac	ac
P-51	+++++	-	
P-52	+++++	-	
P-53	+++++	ac	
P-55	+++++	ac	
P-56	+++++	ac	
P-57	+++++	ac	
P-58	+++++	ac	
P-59	+++++	ac	
P-60	+++++	ac	
P-62	+++++	ac	
P-63	+++++	ac	
P-64	+++++	ac	
P-65	+++++	ac (~ 3%)	
P-66	+++++	ac (~ 3%)	
P-67	+++++	ac	
S-2	ac	+++++	ac
S-3	+++	++ (~ 22%)	+ (~ 6%)
S-4	+++++	ac (~ 2%)	
S-5	++	+++	
S-6	+++	++ ac (~ 14%)	ac
S-7	+++++	ac (~ 3.5%)	
S-8	++++	+	ac
S-9	++++	+ (~ 10%)	

+: relative abundance of mineral, ac- accessory

Table 1. Continued.

sample no	dolomite	calcite	quartz
S-10	+ (~6%)	++++	ac (~4%)
S-11	+++++	ac (~4%)	
S-12	+++++	ac	
S-13	+++++	ac	
S-14	+++++	ac (~3%)	
S-15	+++++	ac (~3%)	
S-17	+++++	-	
S-18	++++	+ (~12%)	
S-19	ac (~4%)	+++++	
S-20	+++++	ac (~4%)	
S-21	+++++	ac	
S-22	+++++	ac	
S-23	ac (~3%)	+++++	
S-25	-	+++++	
S-28	+ (~ 10%)	++++	
S-30	ac	+++++	
Y-3	+++++	-	ac
Y-4	+++++	-	
Y-5	+++++	-	
Y-6	+++++	-	
Y-7	+++++	-	
Y-8	+++++	-	
Y-9	+++++	-	
Y-10	+++++	-	
Y-11	+++++	-	
Y-12	+++++	-	
Y-13	+++++	-	
Y-14	+++++	-	
Y-15	+++++	-	
Y-16	+++++	-	
Y-17	+++++	-	
Y-18	+++++	-	
Y-19	+++++	ac (~4%)	
Y-20	+++++	-	
Y-21	+++++	-	
Y-22	+++++	-	
Y-23	+++++	-	
Y-24	+++++	-	
Y-25	+++++	ac	
Y-26	ac (~ 4%)	+++++	
Y-27	+++++	ac	
Y-28	+++++	-	
Y-29	+++++	ac	
Y-30	ac (~ 3%)	+++++	

Table 2. Chemical compositions of selected samples.

sample no	SiO_2 %	Al_2O_3 %	Fe_2O_3 %	MgO %	CaO %	Na_2O %	K_2O %	Ti_2O %	P_2O_5 %	MnO %	Cr_2O_3 %	Ba ppm	Ni ppm	Sr ppm	Zr ppm	Y ppm	Nb ppm	Sc ppm	LOI %	SUM %
very fine to fine crystalline dolomite (T1–type)																				
P-17	1.19	0.44	0.21	20.87	31.14	0.03	0.09	0.02	0.03	0.01	0.002	10	<20	89	<10	<10	<10	<1	46.0	100.05
P-24	2.73	1.08	0.39	20.86	28.78	0.02	0.28	0.04	0.02	<0.01	0.005	16	<20	78	<10	<10	<10	<1	45.9	100.12
P-33	0.85	0.31	0.15	20.81	30.73	0.01	0.07	0.01	0.04	<0.01	0.009	7	22	77	<10	<10	18	<1	47.0	100.01
S-17	1.30	0.39	0.12	21.81	30.04	0.03	0.08	0.01	0.03	<0.01	<0.001	10	<20	94	14	<10	32	<1	46.1	99.93
Y-6	0.96	0.37	0.13	21.46	29.77	0.07	0.08	0.01	0.03	<0.01	0.006	5	30	72	12	<10	37	<1	47.1	100.01
Y-15	0.72	0.33	0.17	20.22	32.07	0.03	0.07	0.01	0.03	0.01	0.003	9	22	81	16	<10	38	<1	46.2	99.89
Y-16	1.28	0.60	0.23	19.01	33.37	0.04	0.15	0.02	0.03	<0.01	<0.001	6	<20	119	<10	<10	19	1	45.3	100.05
Y-18	0.66	0.20	0.06	21.40	31.26	0.01	0.04	<0.01	0.02	<0.01	0.004	6	31	68	<10	<10	24	<1	46.3	99.98
Y-19	0.69	0.27	0.14	20.07	32.72	0.02	0.05	0.01	0.02	<0.01	0.004	<5	<20	94	<10	<10	13	<1	45.9	99.92
Y-20	1.01	0.51	0.21	21.17	31.16	0.01	0.12	0.02	0.04	0.01	0.006	8	24	75	<10	<10	22	<1	45.7	99.98
coarse crystalline dolomite (T2–type)																				
P-34	0.07	<0.03	0.04	22.12	31.45	0.01	<0.02	<0.01	0.03	<0.01	0.002	<5	<20	22	13	<10	35	<1	46.2	99.96
P-44	0.34	0.13	0.07	22.18	31.33	0.01	<0.02	<0.01	0.03	<0.01	<0.001	<5	<20	65	12	<10	41	<1	45.8	99.93
P-46	0.16	<0.03	<0.04	22.26	30.83	<0.01	<0.02	<0.01	0.05	<0.01	<0.001	6	25	32	26	<10	54	<1	46.6	99.94
P-48	0.21	0.03	0.06	21.72	30.98	<0.01	<0.02	<0.01	0.04	<0.01	0.004	6	20	48	<10	<10	17	1	46.9	99.96
P-51	0.47	0.06	0.06	21.57	30.94	0.02	<0.02	<0.01	0.03	<0.01	0.005	7	25	58	<10	<10	<10	<1	46.8	99.98
P-60	0.33	0.06	0.05	21.88	31.21	0.02	<0.02	<0.01	0.01	<0.01	<0.001	<5	<20	28	<10	<10	16	<1	46.4	99.99
P-61	1.11	0.48	0.16	20.14	32.22	0.04	0.09	0.02	0.02	<0.01	0.004	8	<20	96	<10	<10	14	<1	45.7	100.00
P-66	1.24	0.57	0.23	19.50	32.63	0.04	0.11	0.09	0.02	0.01	0.002	13	<20	121	20	<10	40	<1	45.5	99.97
Y-27	0.27	0.13	0.06	21.59	31.23	<0.01	<0.02	<0.01	0.01	<0.01	<0.001	<5	<20	47	<10	<10	<10	<1	46.6	99.92
coexisting limestone																				
S-9	1.61	0.45	0.20	1.09	52.78	0.02	0.11	0.02	<0.01	0.01	0.001	10	<20	312	<10	<10	<10	<1	43.5	99.83

LOI- loss on ignition

Table 3. Stable isotope compositions of the selected samples.

sample no	wt% dolomite	d18O (PDB)	d13C (PDB)
very fine to fine crystalline dolomite (T1-type)			
P-17	93.3	–0.45	0.81
P-24	89.8	0.21	–0.58
P-33	93.6	–0.06	0.89
Y-6	91.8	–0.42	1.12
Y-15	86.6	–1.79	–0.39
Y-16	88.1	–0.60	–0.48
average		–0.52	0.23
coarse crystalline dolomite (T2-type)			
P-34	92.8	–3.44	1.16
P-44	93.2	–2.55	0.76
P-46	93.5	–3.33	1.00
P-48	93.4	–2.94	–0.26
P-51	89.9	–2.73	0.32
P-60	91.1	–3.32	1.13
P-61	94.6	–1.27	0.98
average		–2.78	0.73
coexisting limestone			
S-9	88.4 (calcite)	–5.44	-0.93

‰ PDB (avg. +0.73 ‰ PDB), respectively. The coexisting limestone sample (S-9) has $\delta^{18}O$ and $\delta^{13}C$ values of –5.44 and –0.93 ‰ PDB, respectively. The T2-type dolomites exhibit more ^{18}O-depleted values relative to the T1-type dolomites, and $\delta^{18}O$ value of the limestone differentiates from values of the dolomite samples.

Discussion

The Lower Liassic carbonates were deposited in a peritidal environment, and then subsequently underwent extensive dolomitization. Two major stages of dolomitization are identified in the carbonate rocks based on the petrographic and geochemical data (Figure 12). The very fine to fine crystalline dolomite (T1) characterizes an early stage formed from seawater by syn-sedimentary replacement of peritidal sediments before lithification (Morrow 1982; Banner *et al.* 1988; Tucker & Wright 1990; Qing 1998; Arenas *et al.* 1999; Balog *et al.* 1999). The syn-sedimentary origin is based on: (1) the bedded character of the early formed dolomites; (2) the lamination of very fine to fine crystalline dolomites with mud-rich intervals; (3) dolomite clasts in intraformational conglomerate; (4) desiccation breccias with dolomite clasts; (5) mud-crack association with T1-type dolomites; and (6) the occurrence of dolomites from prior to stylolitization. The very fine to fine crystalline textures are likely resulted from : (i) slow rates of dolomitization, (ii) original sediment mineralogy and fine texture, and (iii) number of nucleation sites (Mresah 1998). The slow rates may have been controlled by permeability (Dawans & Swart 1988) or low supersaturation (Boistelle 1982). The presence of mud-cracks, desiccation breccias and fenestral pores indicate slightly restricted evaporitic conditions, and the absence of evaporite minerals and/or their relics and $\delta^{18}O$ values suggest dolomitization from low supersaturated or penesaline seawater (Zengzhao *et al.* 1998; Qing *et al.* 2001). The slightly depleted $\delta^{18}O$ values of T1-type dolomites are consistent with this interpretation, and are resulted by their diagenetic stabilitization in either burial or meteoric environments (Land 1985; Yoo & Lee 1998; Zengzhao *et al.* 1998; Reinhold 1998). However, Veizer & Hoefs (1976) and Veizer *et al.* (1999) explain that the wide variations in

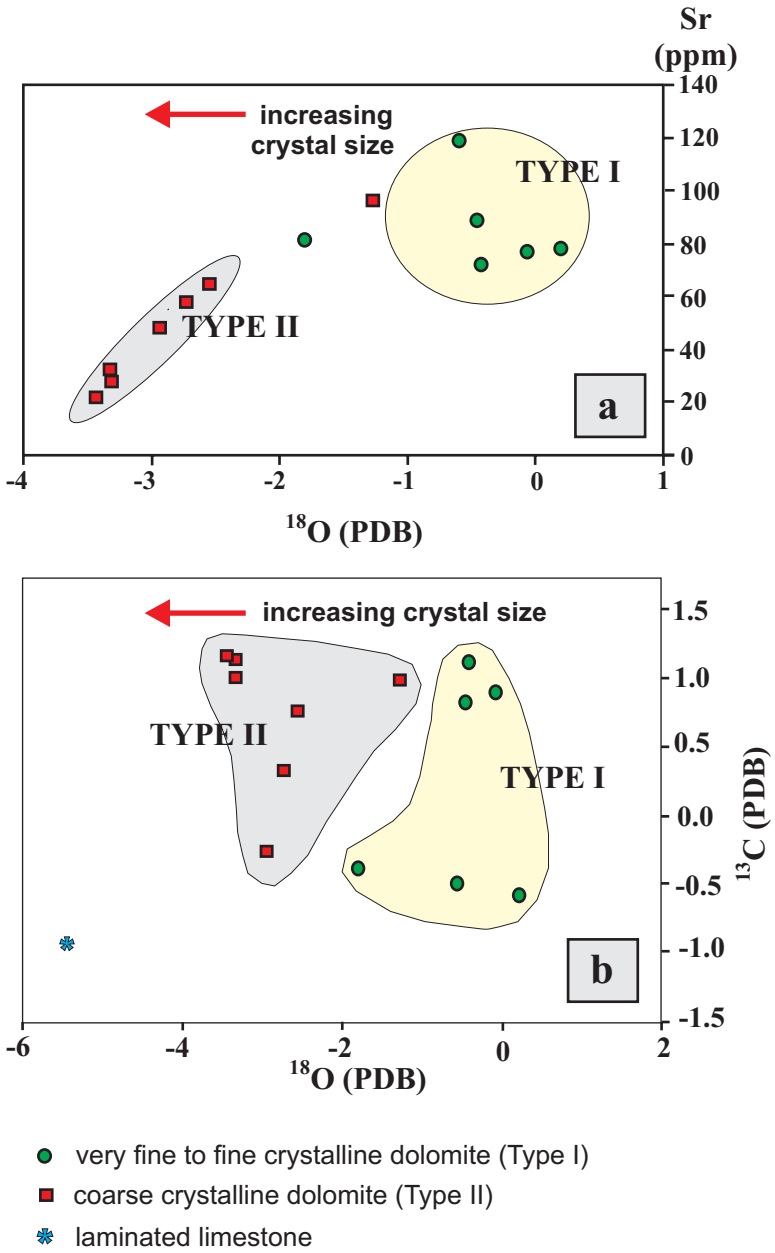

Figure 11. Crossplots of $\delta^{18}O$ versus Sr and $\delta^{13}C$ values. (a) A crossplot of $\delta^{18}O$ versus Sr showing two dolomite-types formed at different stages. Distribution of the T2 dolomite samples (red points) shows a trend where $\delta^{18}O$ and Sr values change covariantly. These changes are inversely related with their crystal size; (b) a crossplot of $\delta^{18}O$ versus $\delta^{13}C$ showing two dolomite-types.

$\delta^{18}O$ and $\delta^{13}C$ values of ancient syn-sedimentary dolomites are related to secular fluctuations in seawater isotopic composition through time. In meteoric environment, $\delta^{18}O$ values of the carbonates tend to be homogeneous because of a ubiquitous source of oxygen (Allan & Matthews 1982) and quite negative (e.g., –6.8 ‰ PDB for mixing zone dolomite, Taylor & Sibley 1986), whereas $\delta^{18}O$ values are more variable during the

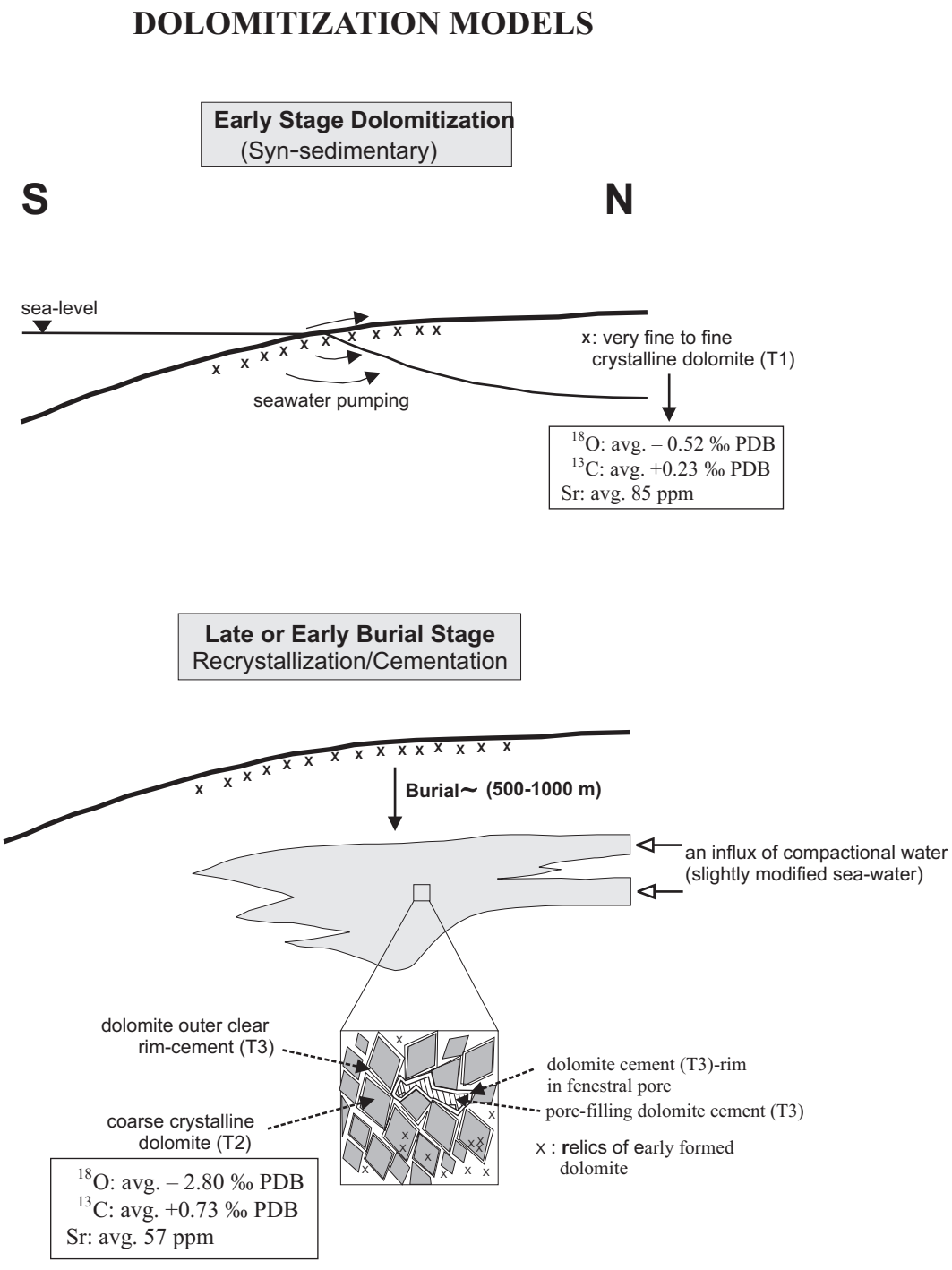

Figure 12. Schematic illustration of the two stage dolomitization: (1) early (syn-sedimentary) and (2) relatively late (post-depositional or early burial).

progressive burial (Tucker & Wright 1990). The similar oxygen isotope values for syn-sedimentary dolomites are reported in the literature (Zengzhao *et al.* 1998; Qing 1998; Balog *et al.* 1999; Auajjar & Bouleque 2003; Varol & Matsumato 2005). The thin-section examination shows that the samples with relatively $\delta^{18}O$-depleted values are associated with relatively larger crystal sizes (close to upper size limit of the group) due to the partial recrystallization during progressive burial. This interpretation is also supported by the absence of dissolution moldics and vugs. Considering the oxygen isotope fractionation value of 3 ± 1 ‰ PDB between dolomite and calcite (Land 1980), we can conclude that the $\delta^{18}O$ value (–5.44 ‰ PDB) of coexisting limestone based on the geochemical data is consistent with late dolomites, and suggests chemical changes during the burial diagenesis. However, X-ray diffractogram of sample S-9 suggests dolomite or limy dolomite rock-type. Difference in results is due to sampling and variation in the sample. The $\delta^{13}C$ values are more typical than the $\delta^{18}O$ values for the syn-sedimentary dolomites (Auajjar & Bouleque 2003), indicating that the $\delta^{13}C$ values are retained from the precursor marine carbonates (Land 1980). The $\delta^{13}C$ values of Lower Jurassic marine carbonates average ~1.5‰ PDB, which is similar or slightly greater than that of modern marine carbonates (~0 to 1‰ PDB; Allan & Matthews 1977; Holser 1984; Popp *et al.* 1986; Lohman & Walker 1989; Veizer *et al.* 1999). Land (1985) concluded that seawater is the only widely available fluid with sufficient magnesium to cause massive dolomitization. Dolomitization and Mg transport were possibly related to a daily pumping of supersaturated marine fluids through the peritidal sediments and some degree of vertical pumping of fluids (Carballo *et al.* 1987; Mazzullo *et al.* 1995). The precursor sediments of this early dolomitization were predominantly micrite which provides favourable substrates for dolomitization because the high surface area provides abundant potential nucleation sites (Sibley 1982).

Dolomite (T2) and (T3) are interpreted to have formed late in diagenetic history, indicating the post-depositional or early burial stage (Banner *et al.* 1988; Qing 1998; Balog *et al.* 1999; Qing *et al.* 2001) whereby dolomite T2 formed by recrystallization of early dolomites (Land 1985; Hardie 1987; Banner *et al.* 1988; Machel 1997; Qing 1998; Reinhold 1998; Al-Aasm & Packard 2000; Chen *et al.* 2004) at slightly increased temperatures, and subsequently dolomite T3 precipitated as a cement. The evidence for possible recrystallization of early dolomites (Machel 1997) are: (1) relics of early dolomites in the intercrystalline areas and also in the large euhedral crystals; (2) loss of original texture; (3) an increase in crystal size, MgO content and slight cation ordering; (4) euhedral crystal shapes; (5) relatively low Sr values; and (6) a shift toward the lighter $\delta^{18}O$ values of coarse crystalline dolomite (T2). The oxygen isotopic fractionation between water and carbonates is highly temperature-dependent (Friedman & O'Neil 1977 and many others). Therefore, burial temperatures of the late dolomites (T2) can be estimated using the Fritz & Smith (1970) expression given in Dickson & Coleman (1980):

$$T\ ^{o}C = 31.9 - 5.55\ (\delta d - \delta w) + 0.17\ (\delta d - \delta w)^2$$

where T is temperature in Celsius, dd and dw are oxygen isotopic composition of dolomite and formation water (modified sea water; Land 1985) in PDB scale. Assuming a constant $\delta^{18}O_{seawater}$ value of –0 ‰ SMOW (Tucker & Wright 1990; Rosales *et al.* 2004), the calculated temperatures for the late dolomitization range from 39 to 53 °C based on oxygen isotope values of dolomite T2 (Hardie 1987; Qing 1998; Reinhold 1998). These temperatures require subsurface depths of roughly 500 to 1000 m, assuming a surface temperature of 20 °C and a geothermal gradient of 30 °C / km (Allen & Allen 1990; Eren 1993). Burial at ~500 m depth is enough to raise the temperature of pore waters sufficiently to effect dolomitization (Qing *et al.* 2001). Taking a consideration of the secular variation in dw, we need to re-evaluate the our estimations according to $\delta^{18}O$ value of the Early Jurassic seawater which is lighter than the recent seawater (Veizer *et al.* 1999). In the literature, a δ_{water} value of ~ -1.0 ‰ SMOW seems reasonable for the Early Jurassic seawater (Reinhold 1998; Haas & Demeny 2002; Rosales *et al.* 2004). The use of this $\delta^{18}Ow$ value results the burial temperatures from 33 to 46 °C. In the both cases, the temperature estimations include many uncertainties such as sampling, analytical errors, diagenetic factors, etc. The first temperature estimates seem to be more realistic than the second estimated values. The $\delta^{13}C$ values of the early and late dolomites are almost the same, that may indicate marine-derived warm

dolomitizing fluids. These warm fluids were probably oxidizing in character (Qing 1998) because of staining of dolomite cements which are nonferroan. In the early burial dolomitization, the main source of Mg is the early dolomites (T1), and additional Mg is provided from the modified seawater. Geochemically, dolomitization is favoured at elevated burial temperatures because the kinetic inhibitions act at low temperatures less than 50 °C (Machel & Mountjoy 1986; Hardie 1987; Tucker 1991; Budd 1997). Therefore, the recrystallization took place at elevated burial temperatures, and resulted an increase in crystal size and slight cation ordering to form the coarse crystalline dolomites (T2) and changes in isotope geochemistry and trace element contents of early dolomites (T1). The dolomite T1 is calcium rich and poorly ordered, so characterizing the highly metastable phase (Land 1985). The covariant trend of $\delta^{18}O$ and Sr values inversely related to cyrstal size (Figure 11a) suggests progressive recrystallization. The geometry of dolomite T2 and the absence or poor development of coarse crystalline dolomites in the Soğuksu section (Figure 7) suggests an influx of laterally percolating fluids from landward, resulting from compaction (Qing 1998). The late dolomitization occurred before any significant loss of porosity and permeability hindered fluid circulation through the sediment evidenced by well preservation of primary pores (Warren 2000).

Conclusions

In the Lower Liassic carbonates, two major stages of dolomitization are distinguished on the basis of petrographic and geochemical characteristics. In the early stage, very fine to fine crystalline dolomites (T1) formed from penesaline seawater by syn-sedimentary replacement of peritidal sediments before lithification. In the late stage, the coarse crystalline dolomites (T2) formed as a result of the recrystallization of less stoichiometric dolomite T1, and subsequently dolomite cement (T3) precipitated in the pores and around the dolomite rhomb(s) as a clear outer rim from the same dolomitizating fluid (modified seawater) at elevated burial temperatures. The recrystallization caused an increase in crystal size, a shift to more negative values in $\delta^{18}O$ and low Sr contents in the dolomites. But the $\delta^{13}C$ values do not exhibit a significant change during the later diagenetic modification.

Acknowledgement

The authors are grateful to Roman Koch from Erlangen University, Germany and two anonymous reviewers of the journal for their constructive comments to improve the paper. Appreciation is extended to Erdin Bozkurt (Editor in Chief) for his comments and editorial suggestions. John A. Winchester helped with the English of the final text. This study represents further work on a master's thesis completed by the second author, which was financially supported by the Mersin University Research Fund under Project no: BAP-FBE JM (MY) 2003-2 YL.

References

Adamia, S., Bergougnan, H., Fourquin, C., Haghipour, A., Lordkipanidze, M.B., Özgül, N., Ricou, L.E. & Zakariadze, G.S. 1980. The Alpine Middle East between the Aegean and the Oman traverses. *In*: Aubouin, J., Debelmas, J. & Latreille, M. (eds), *Texte Integral du Colloque C.5 Geologie des Chaines Alpines Issues de la Tethys*. Publications de 26e Congres Geologique International, Paris, 122–136.

Allan, J.R. & Matthews, R.K. 1977. Carbon and oxygen isotopes as diagenetic and stratigraphic tools: data from surface and subsurface of Barbados, West Indies. *Geology* **5**, 16–20.

Allan, J.R. & Matthews, R.K. 1982. Isotope signatures associated with early meteoric diagenesis. *Sedimentology* **29**, 797–817.

Allen, P.A. & Allen, J.R. 1990. *Basin Analysis: Principles and Applications*. Blackwell Scientific Publications, Oxford.

Arenas, C., Alonso Zarza, A.M. & Pardo, G. 1999. Dedolomitization and other early diagenetic processes in Miocene lacustrine deposits, Ebro Basin (Spain). *Sedimentary Geology* **125**, 23–45.

Al-Aasm, I.S. & Packard, J.J. 2000. Stabilization of early-formed dolomite: a tale of divergence from two Mississippian dolomites. *Sedimentary Geology* **131**, 97–108.

Auajjar, J. & Boulegue, J. 2003. Dolomitization patterns of the Liassic platform of the Tazekka Pb-Zn district, Taza, eastern Morocco: petrographic and geochemical study. *Journal of South American Earth Sciences* **16**, 167–178.

Balog, A., Read, F. & Haas, J. 1999. Climate-controlled early dolomite, late Triassic cyclic platform carbonates, Hungary. *Journal of Sedimentary Research* **69**, 267–282.

BANNER, J.L., HANSON, G.N. & MEYERS, W.J. 1988. Water-rock interaction history of regionally extensive dolomites of the Burlington-Keokuk Formation (Mississippian): isotopic evidence. *In*: SHUKLA, V. & BAKER, P.A. (eds), *Sedimentology and Geochemistry of Dolostones*. Society of Economic Paleontologists and Mineralogists, Special Publications **43**, 97–113.

BEHRENS, E.W. & LAND, L.S. 1972. Subtidal Holocene dolomite, Baffin Bay, Texas. *Journal of Sedimentary Petrology* **42**, 155–161.

BOISTELLE, R. 1982. Mineral crystallization from solutions. *Estudios Geologicos* **38**, 135–153.

BOZKURT, E. 2001. Neotectonics of Turkey – a synthesis. *Geodinamica Acta* **14**, 3–30.

BRINDLEY, G.W. 1980. Quantitative X-ray analysis of clays. *In*: BRINDLEY, G.W. & BROWN, G. (eds), *Crystal Structures of Clay Minerals and Their X-ray Identification*. Mineralogical Society Monograph **5**, 411–438.

BUDD, D.A. 1997. Cenozoic dolomites of carbonate islands: their attributes and origin. *Earth Science Reviews* **42**, 1–47.

CARBALLO, J.D., LAND, L.S. & MISER, D.E. 1987. Holocene dolomitization of supratidal sediments by active tidal pumping, Sugarloaf Key, Florida. *Journal of Sedimentary Petrology* **57**, 153–165.

CHEN, D., QING, H. & YANG, C. 2004. Multistage hydrothermal dolomites in the Middle Devonian (Givetian) carbonates from the Guilin area, South China. *Sedimentology* **51**, 1029–1051.

DAWANS, J.M. & SWART, P.K. 1988. Textural and geochemical alternations in Late Cenozoic Bahamian dolomites. *Sedimentology* **35**, 385–403.

DEMİRTAŞLI, E., TURHAN, N., BİLGİN, A.Z. & SELİM, M. 1984. Geology of the Bolkar mountains. *In*: TEKELİ, O. & GÖNCÜOĞLU, M.C. (eds), *Geology of the Taurus Belt*. Proceedings of International Tauride Symposium. Mineral Research and Exploration Institute (MTA) of Turkey Publications, 125–141.

DEWEY, J.F., PITMANN, W.C., RYAN, W.B.F. & BOWIN, J. 1973. Plate tectonic evolution of the Alpine system. *Geological Society of America Bulletin* **84**, 3137–3180.

DICKSON, J.A.D. 1966. Carbonate identification and genesis as revealed by staining. *Journal of Sedimentary Petrology* **36**, 491–505.

DICKSON, J.A.D. & COLEMAN, M.L. 1980. Changes in carbon and oxygen isotope composition during limestone diagenesis. *Sedimentology* **27**, 107–118.

EREN, M. 1993. Burial dolomitization within Atoka carbonates. *Giornale di Geologia* **55**, 171–176.

EREN, M., TASLI, K. & TOL, N. 2002. Sedimentology of Liassic carbonates (Pirencik Tepe measured section) in the Aydıncık (İçel) area, southern Turkey. *Journal of Asian Earth Sciences* **20**, 791–801.

FRIEDMAN, I. & O'NEIL, J.R. 1977. Compilation of stable isotope factors of geochemical interest. *In*: FLEISCHER, M. (ed), *Data of Geochemistry*. United States Geological Survey Professional Paper **440-KK**, 1–12.

FRITZ, P. & SMITH, D.G.W. 1970. The isotopic composition of secondary dolomite. *Geochimica et Cosmochimica Acta* **34**, 1161–1173.

GINSBURG, R.N. 1975. *Tidal Deposits: A Casebook of Recent Examples and Fossil Counterparts*. Springer-Verlag, Berlin.

GOLDSMITH, J.R., GRAF, D.L. & HEARD, H.C. 1961. Lattice constants of the calcium-magnesium carbonates. *American Mineralogists* **46**, 453–457.

GÜNDOĞDU, M.N. 1982. *Geological, Mineralogical and Geochemical Investigation of the Bigadiç Neogene Sedimentary Basin*. PhD Thesis, Hacettepe Universty, Ankara [in Turkish with English abstract, unpublished].

HAAS, J. & DEMENY, A. 2002. Early dolomitisation of Late Triassic platform carbonates in the Transdanubian Range (Hungary). *Sedimentary Geology* **151**, 225–242.

HALLEY, R.B. 1975. Peritidal lithologies of Cambrian carbonate islands, Carrara Formation, Southern Great Basin. *In*: GINSBURG, R.N. (ed), *Tidal Deposits*. Springer-Verlag, Berlin, 279–288.

HARDIE, L.A. 1987. Dolomitization: a critical view of some current views. *Journal of Sedimentary Petrology* **57**, 166–183.

HARDY, R. & TUCKER, M. 1995. X-ray powder diffraction of sediments. *In*: TUCKER, M. (ed), *Techniques in Sedimentology*. Blackwell Science, Oxford, 191–228.

HOLSER, W.T. 1984. Gradual and abrupt shifts in ocean chemistry during Phanerozoic time. *In*: HOLLAND, H.D. & TRENDALL, A.F. (eds), *Patterns of Change of Earth Evolution*. Springer-Verlag, Berlin, 171–205.

KABAL, Y. & TASLI, K. 2003. Biostratigraphy of the lower Jurassic carbonates from the Aydıncık area (Central Taurides, S Turkey) and morphological analysis of *Lituolipora Termieri* (Hottinger, 1967). *Journal of Foraminiferal Research* **33**, 338–351.

KETİN, İ. 1966. Tectonics units of Anatolia (Asia Minor). *Mineral Research and Exploration Institute (MTA) of Turkey Bulletin* **66**, 23–34.

KOÇ, H. 1996. *Stratigraphy and Geotectonic Interpretation of Aydıncık (IÇEL) Area*. MSc Thesis, Mersin University [in Turkish, unpublished].

KOÇ, H., ÖZER, E. & ÖZSAYAR, T. 1997. Geology of Aydıncık (İçel) area. *Geosound: Earth Sciences* **30**, 417–427 [in Turkish with English abstract].

KOÇ, H., ÜNLÜGENÇ, U.C. & ÖZER, E. 2005. Tectono-stratigraphical investigation of an area between Aydıncık-Bozyazı (Mersin). *Geological Society of Turkey Bulletin* **48**, 1–26 [in Turkish with English abstract].

LAND, L.S. 1980. The isotopic and trace element geochemistry of dolomite: the state of the art. *In*: ZENGER, D.H. & ETHINGTON, R.L. (eds), *Concept and Models of Dolomitization*. Society of Economic Paleontologists and Mineralogists, Special Publications **28**, 87–110.

LAND, L.S. 1985. The origin of massive dolomite. *Journal of Geological Education* **33**, 112–125.

LOHMANN, K.C. & WALKER, J.C.G. 1989. The d^{18}O record of Phanerozoic abiotic marine calcite cements. *Geophysical Research Letters* **16**, 319–322.

MACHEL, H.G. 1997. Recrystallization versus neomorphism, and the concept of significant recrystallization in dolomite research. *Sedimentary Geology* **113**, 161–168.

MACHEL, H.G. & MOUNTJOY, E.W. 1986. Chemistry and environments of dolomitization – A reappraisal. *Earth Science Reviews* **23**, 175–222.

MAZZULLO, S.J., BISCHOFF, W.D. & TEAL, C.S. 1995. Holocene shallow-subtidal dolomitization by near-normal seawater, northern Belize. *Geology* **23**, 341–344.

MORROW, D.W. 1982. Diagenesis II. Dolomite-Part II. Dolomitization models and ancient dolostones. *Geoscience Canada* **9**, 95–107.

MRESAH, M.H. 1998. The massive dolomitization of platformal and basinal sequences: proposed models from the Paleocene, Northeast Sirte Basin, Libya. *Sedimentary Geology* **116**, 199–226.

ÖZGÜL, N. 1984. Stratigraphic and tectonic evolution of the central Taurides. *In*: TEKELI, O. & GÖNCÜOĞLU, M.C. (eds), *Geology of the Taurus Belt*. Proceedings of International Tauride Symposium. Mineral Research and Exploration Institute (MTA) of Turkey Publications, 77–90.

PARK, R. 1976. A note on the significance of lamination in stromatolites. *Sedimentology* **23**, 379–393.

POPP, B.N., ANDERSON, T.F. & SANBERG, P.A. 1986. Brachiopods as indicators of original isotopic compositions in some Paleozoic limestones. *Geological Society of America Bulletin* **97**, 1262–1269.

QING, H. 1998. Petrography and geochemistry of early-stage, fine- and medium-crystalline dolomites in the Middle Devonian Presqu'ile Barrier at Pine Point, Canada. *Sedimentology* **45**, 433–446.

QING, H., BOSENCE, D.W.J. & ROSE, E.P.F. 2001. Dolomitization by penesaline sea water in Early Jurassic peritidal platform carbonates, Gibraltar, western Mediterranean. *Sedimentology* **48**, 153–163.

REINHOLD, C. 1998. Multiple episodes of dolomitization and dolomite recrystallization during shallow burial in Upper Jurassic shelf carbonates: eastern Swabian Alb, southern Germany. *Sedimentary Geology* **121**, 71–95.

ROBERTSON, A. 1998. Mesozoic–Tertiary tectonic evolution of the east Mediterranean area: relevance to Turkish geology. *The Third International Turkish Geology Symposium*. Middle East Technical University, Ankara, Abstracts, p.16.

ROSALES, I., QUESADA, S. & ROBLES, S. 2004. Paleotemperature variations of Early Jurassic seawater recorded in geochemical trends of belemnites from the Basque-Cantabrian basin, northern Spain. *Palaeogeography, Palaeoclimatology, Palaeoecology* **203**, 253–275.

ŞENGÖR, A.M.C. & YILMAZ, Y. 1981. Tethyan evolution of Turkey: a plate tectonic approach. *Tectonophysics* **75**, 181–241.

ŞENGÖR, A.M.C., YILMAZ, Y. & SUNGURLU, O. 1984. Tectonics of the Mediterranean Cimmerides: nature and evolution of the western termination of Paleo-tethys. *In*: DIXON, J.E. & ROBERTSON, A.H.F. (eds), *Evolution of Eastern Mediterranean*. Geological Society, London, Special Publications **13**, 117–152.

SIBLEY, D.F. 1982. The origin of common dolomite fabrics: clues from the Pliocene. *Journal of Sedimentary Petrology* **52**, 1087–1100.

TAYLOR, T.R. & SIBLEY, D.F. 1986. Petrographic and geochemical characteristics of dolomite types and the origin of ferroan dolomite in the Trenton Formation, Ordovician, Michigan Basin, USA. *Sedimentology* **33**, 61–86.

THERIAULT, F. & HUTCHEON, I. 1987. Dolomitization and calcitization of the Devonian Grosmont Formation, northern Alberta. *Journal of Sedimentary Petrology* **57**, 955–966.

TUCKER, M.E. 1991. *Sedimentary Petrology: An Introduction to the Origin of Sedimentary Rocks*. Blackwell Science, Oxford.

TUCKER, M.E. & WRIGHT, V.P. 1990. *Carbonate Sedimentology*. Blackwell Science, Oxford.

VAROL, B. & MATSUMOTO, R. 2005. Early and late dolomites in the carbonate platform: An example from Middle Devonian carbonates of the Taurus Mountains, south-central Turkey. *Neues Jahrbuch für Mineralogie-Abhandlungen* **181**, 135–145.

VEIZER, J., ALA, D., AZMY, K., BRUCKSCHEN, P., BUHL, D., BRUHN, F., CARDEN, G.A.F., DIENER, A., EBNETH, S., GODDERIS, Y., JASPER, T., KORTE, C., PAWELLEK, F., PODLAHA, O.G. & STRAUSS, H. 1999. ^{87}Sr/^{86}Sr, d^{13}C and d^{18}O evolution of Phanerozoic seawater. *Chemical Geology* **161**, 59–88.

VEIZER, J. & HOEFS, J. 1976. The nature of ^{18}O/^{16}O and ^{13}C/^{12}C secular trends in sedimentary carbonate rocks. *Geochimica et Cosmochimica Acta* **40**, 1387–1395.

WARREN, J. 2000. Dolomite: occurrence, evolution and economically important associations. *Earth Science Reviews* **52**, 1–81.

YEŞİLOT, M. 2005. *Origin of Lower Liassic dolomites in Aydıncık/Mersin Area*. MSc Thesis, Mersin University [in Turkish with English abstract, unpublished].

YOO, C.M. & LEE, Y.I. 1998. Origin and modification of early dolomites in cyclic shallow platform carbonates, Yeongheung Formation (Middle Ordovician), Korea. *Sedimentary Geology* **118**, 141–157.

YÜKSEL, M.M. 1985. *Geology of the Aydıncık (İçel) Region*. MSc Thesis, Middle East Technical University [unpublished].

ZENGZHAO, F., YONGSHENG, Z. & ZHENKUI, J. 1998. Type, origin, and reservoir characteristics of dolostones of the Ordovician Majiagou Group, north China Platform. *Sedimentary Geology* **118**, 127–140.

Received 24 March 2006; revised typescript received 13 October 2006; accepted 02 February 2007